Folded graphene nanochannels via pulsed patterning of graphene

Ive Silvestre, Arthur W. Barnard, Samantha P. Roberts, Paul L. McEuen, and Rodrigo G. Lacerda

Citation: Appl. Phys. Lett. **106**, 153105 (2015); doi: 10.1063/1.4918683
View online: http://dx.doi.org/10.1063/1.4918683
View Table of Contents: http://aip.scitation.org/toc/apl/106/15
Published by the American Institute of Physics

Folded graphene nanochannels via pulsed patterning of graphene

Ive Silvestre,[1,2] Arthur W. Barnard,[3] Samantha P. Roberts,[2] Paul L. McEuen,[2] and Rodrigo G. Lacerda[1,2]
[1]*Departamento de Física, ICEx, Universidade Federal de Minas Gerais, Caixa Postal 702, CEP 30161-901, Belo Horizonte, Minas Gerais, Brazil*
[2]*Department of Physics, Cornell University, Ithaca, New York 14853, USA*
[3]*School of Applied and Engineering Physics, Cornell University, Ithaca, New York 14853, USA*

(Received 7 January 2015; accepted 9 April 2015; published online 17 April 2015)

We present a resist-free patterning technique to form electrically contacted graphene nanochannels via localized burning by a pulsed white light source. The technique uses end-point detection to stop the burning process at a fixed resistance to produce channels with resistances of 10 kΩ to 100 kΩ. Folding of the graphene sheet takes place during patterning, which provides very straight edges as identified by AFM and SEM. Electrical transport measurements for the nanochannels show a non-linear behavior of the current vs source-drain voltage as the resistance goes above 20 kΩ indicating conduction tunneling effects. Electrochemical gating was performed to further electrically characterize the constrictions produced. The method described can be interesting not only for fundamental studies correlating edge folded structures with electrical transport but also as a promising path for fabricating graphene devices *in situ*. Additionally, this method might also be extended to create nanochannels in other 2D materials. © *2015 AIP Publishing LLC*.
[http://dx.doi.org/10.1063/1.4918683]

Since the isolation of graphene in 2004[1] by micromechanical exfoliation of graphite, its electronic, mechanical, and structural properties have been studied extensively.[2–6] With the advent of chemical vapor deposition (CVD) techniques, large-area single layer graphene (SLG) became available,[7–9] making possible top-down device architectures where the graphene is patterned into desired shapes. Patterning graphene into nanochannels is a pathway to high performance electronics[10,11] and is also interesting for biosensing applications such as DNA sequencing.[12] One challenge is controlling the properties of the edges of these structures, which can lead to strong disorder. On the other hand, the production of folded edges has been predicted as an alternate way to modify graphene electronic structure and enhance its mechanical properties.[13–20]

Recently, the ablation of graphene by ultra-short laser pulses has been demonstrated, and this technique often generates folded graphene edges;[21–25] however, so far the previous works have been focused on either the patterning of graphene into microribbons or on the understanding of the ablation process itself. Differently, here, we used this approach to achieve folded graphene nanochannels down to 30 nm in width with controllable resistance ranging from 10 kΩ to 100 kΩ. A focused pulsed laser is scanned along the graphene to define a cut while simultaneously employing end-point detection to turn off the laser when a desired resistance is reached. Additionally, we also have performed a detailed structural analysis (by Scanning Electron Microscopy (SEM), Atomic Force Microscopy (AFM), and TEM) of the morphology of the folded structures produced, as well as nonlinear electrical measurements and electrolyte gating to further characterized the nanochannels.

We start by describing the sample preparation. Graphene is grown on Cu foils inside a CVD chamber at 1000 °C and low pressure of H_2/CH_4 ($P_{total} = 0.12$ Torr). A 150 nm thick layer of PMMA is spun on top of the graphene/Cu surface, and Cu is then etched away. After cleaning in several DI water baths, the PMMA/graphene structure is transferred onto the appropriate substrate. The PMMA is then removed using solvents.

We first characterize the laser ablation process. CVD graphene is transferred from the Cu substrate onto a 10 nm SiN/Si TEM grid. As shown in Fig. 1(a), light from a nanosecond supercontinuum white light source (repetition rate $f = 25$ kHz and pulse width 1–2 ns) is ported into an inverted

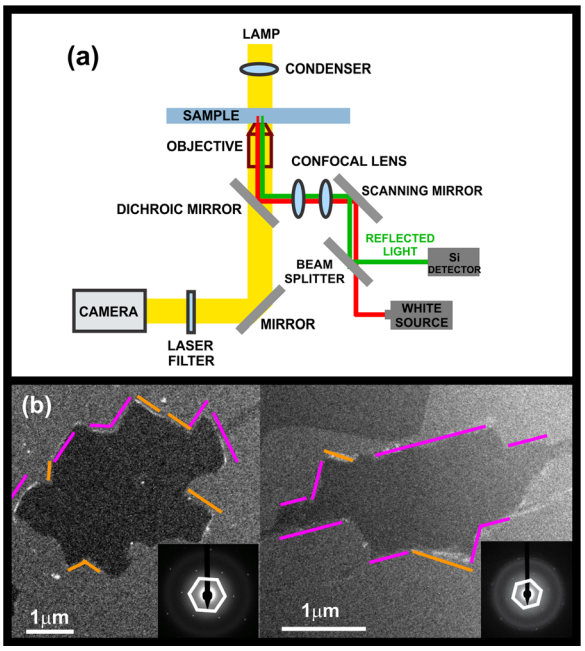

FIG. 1. (a) Sketch of the experimental set-up. (b) DF-TEM images for laser burnt areas of graphene on top of SiN grid. The inset shows the diffraction pattern of the graphene from where the indexing method for the zigzag (orange) and armchair (magenta) directions are deduced.

microscope and focused onto the graphene sample using a 40× Olympus objective with NA = 0.9. Piezo-controlled scanning mirrors are used to position the beam on the sample with a minimum step size of 30 nm via a software interface.[26]

Figure 1(b) shows Dark-field Transmission Electron Microscopy (DF-TEM) images[27] of two ablated regions of graphene on the top of the SiN grid created by a diffraction-limit spot and an energy of 4 μJ per pulse. Micron-scale holes are observed, with the boundary showing curled/folded edges as reported previously.[25] Also shown are the electron diffraction patterns used to determine the crystallographic orientation of the graphene. We label zigzag edges with orange lines and armchair edges with magenta lines. These results suggest that a high density of both armchair and zigzag edges might be generated during the cutting process, consistent with work that studied e-beam induced crack propagation and observed preferential tearing along zigzag and armchair directions.[28] Thus, this ablation method could be a possible path to producing crystallographically-oriented edges. However, it is also important to say, that we are not looking at the edges at atomic resolution, so on the atomic scale, the edges can be a mixture of zigzag and armchair as well be rough still.[29]

We next use this laser ablation technique to pattern electronic devices, as shown schematically in Fig. 2(a). First, CVD graphene is transferred onto a 170 μm thick double-side-polished fused silica chip (25 × 25 mm^2) containing approximately 30 pre-patterned Ti/Au source/drain electrode pairs. A photolithography step (which includes a new layer of PMMA and photoresist) is used to pattern the graphene into rectangular (45 × 63 μm^2) regions that connect the source-drain electrodes. Finally, PMMA/photoresist is removed with solvents and thermal treatment (50% Ar/H_2–300 °C for 4 h). The typical resistance for the completed graphene devices range from 0.8 to 3 kΩ.

The procedure for laser-patterning of these devices is as follows: the laser spot is positioned at one edge of the sample, then moved toward the center of the sheet while the device resistance is monitored via a LabView program interface. When a setpoint value of resistance is reached, the laser is shut off. A second cut is then made from the opposite direction using a larger resistance set-point. The process can be repeated as desired, narrowing the graphene into a nanochannel of a desired resistance. The resistance versus time during fabrication of a device with a final resistance of 100 kΩ is shown in Fig. 2(b). The lower portion of the figure indicates the state of the laser beam. The resistance is stable when the laser is off, but grows continuously as the laser cuts the graphene. Resistances in the range of 10–100 kΩ are reproducibly achievable. It is possible to obtain resistances in the MΩ range though such devices are often unstable.

Figure 2(c) depicts SEM images of typical nanochannels produced by this process. The darker features at the edges of the cuts indicate graphene folded structures. AFM images (not shown) also reveal the formation of folded edges in these devices. Using AFM and SEM images, we correlated the resistance of the constriction with its width. Resistances in the range of 10–20 kΩ corresponded to widths of 100–200 nm, whereas resistances >50 kΩ corresponded to widths of 50–100 nm.[30,31] The width of samples with the highest resistance (in the MΩ range) were too small to be measured.

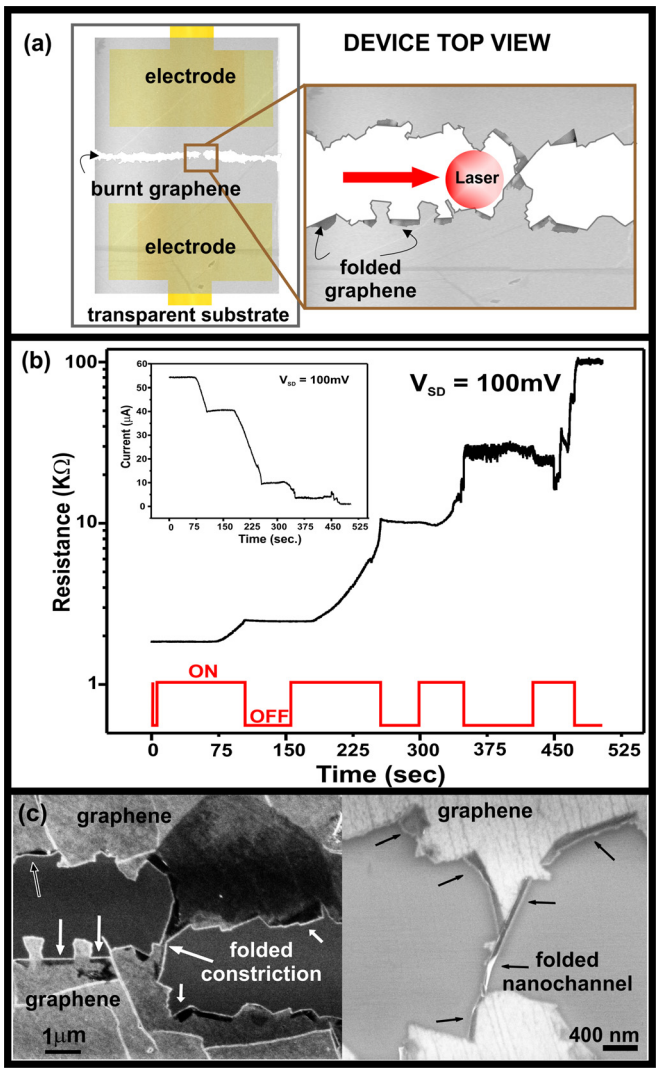

FIG. 2. (a) Sketch of CVD graphene patterned on top of Ti/Au electrodes showing the laser path on both sides. Top view and side view of the cutting procedure, also depicting the folding process of graphene layers. (b) Resistance vs time behavior for a 100 kΩ constriction at 100 mV bias. The inset shows the correspondent current vs time behavior for the same structure. The red diagram indicates the on/off laser state that can be set via a resistance setpoint value. (c) SEM image of two opposite cuts that produce a folded nanoconstriction (left) and nanochannel (right) in the graphene sheet.

The I-V curves for devices before and after cutting are shown in Fig. 3. Before cutting, the behavior is linear, as shown in Fig. 3(a). After cutting, the *I-V* curve becomes increasingly nonlinear as the device resistance grows, as seen in Figs. 3(b) and 3(c) for an 80 kΩ and 300 kΩ channel, respectively (where the resistance was measured at 100 mV bias). This behavior suggests that the constriction is behaving as a tunnel barrier for current flow. This is further supported by the fact that the resistances are significantly higher than for a single spin-degenerate channel, $h/2e^2 = 12$ kΩ. The non-linear behavior found for our samples is consistent with others reported in literature both for very confined graphene bridges[32–35] and nanogaps formed when graphene junctions undergo electrical breakdown.[36] As a final probe of the electronic properties, we use electrochemical gating with a 10 mM KCl ionic solution to change the charge density in

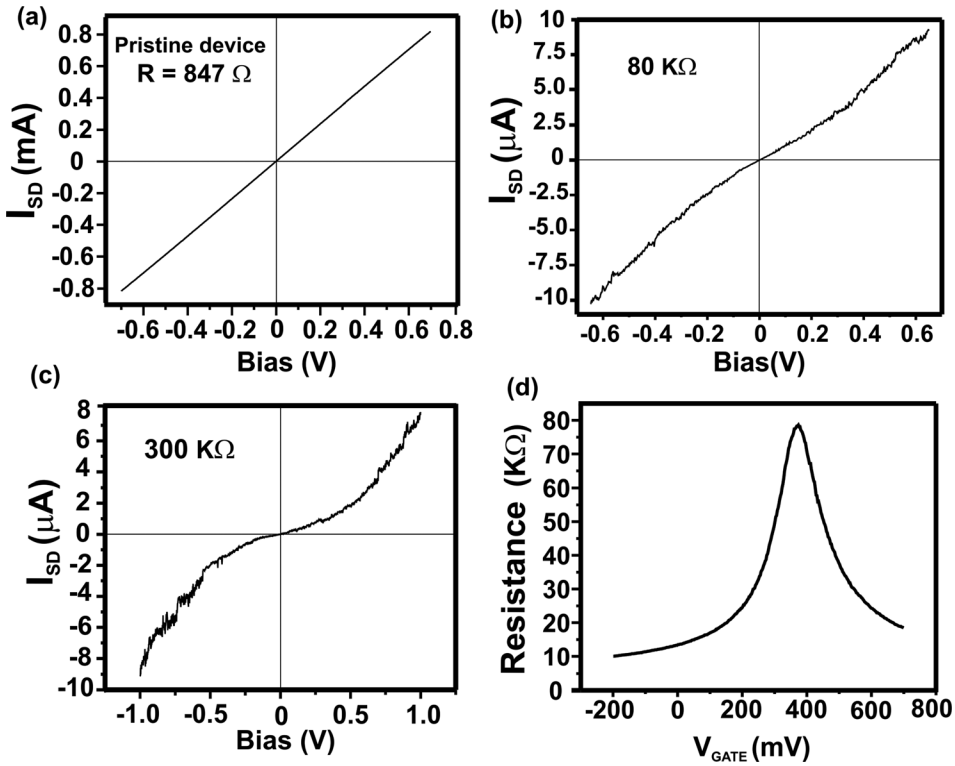

FIG. 3. (a) Linear I-V curve for a pristine graphene device. (b) and (c) Nonlinear I-V curve at room temperature for an 80 kΩ and 300 kΩ graphene nanochannel, respectively. (d) Electrochemical gate-voltage dependence for a graphene nanochannel.

the device. Typical behavior for the conductance versus electrolyte voltage is given in Fig. 3(d), showing a maximum in the resistance at the Dirac point. This is similar to nanochannel devices fabricated by standard lithographic techniques.

If the high resistance and electrical non-linear behavior were due to the formation of a nanogap in the graphene and tunneling across this gap, a gate dependence of the conductance would not be expected.[36] Consequently, the non-linear behavior observed should be related to the formation of barriers within the graphene. The origin of such barriers in graphene constrictions and nanoribbons has been the subject of intense debate. Mechanisms proposed include the opening of an energy band gap due to confinement effects (for widths < 10 nm), the formation of series of quantum dots due to a disorder potential,[32,37–39] and/or Anderson localization.[40] Non-linear tunable transport has also been observed due to localized states on graphene/graphene oxide/graphene junctions and by defect induced localization in graphene constrictions.[35,41]

In fact, the non-linear behavior found in our folded channels is very similar to the ones reported in Ref. 34. In this work, the authors have produced nanochannels with different defect densities. The electrical behavior of the nanochannels shows a non-linear behavior as the defect density increases. For nanochannels with high defect densities, a strong suppression of the conductance with the back gate voltage was also observed. The authors conclude that electrical characteristics are dominated by strong localization of the carriers even at room temperature and that the embedded low-defect density induced a metal-insulator transition. However, a deeper study must be performed in our samples to better clarify the non-linear behavior observed, which was not the scope of the present work.

In conclusion, we present a method to produce folded graphene nanochannels with a controllable resistance using a laser ablation technique. In our measurements, the laser step size was 30 nm, which ultimately set the limit of the channel width. This suggests that this technique can likely be pushed further to make even narrower channels. The cutting process can be performed in a variety of different environments (liquid, gas, etc), opening up interesting new possibilities in manipulating the chemistry of the graphene edges created *in situ*, as well as in introducing intercalating compounds within the graphene folds. Finally, this method could also be applied to produce nanochannels/nanoconstrictions in other 2D materials.[42]

The authors acknowledge Wan Li for helpful discussions and Pinshane Y. Huang for helping with the TEM measurements and analysis. The authors also acknowledge support from the Brazilian agencies: CAPES, CNPq, and FAPEMIG. Device fabrication was performed at the Cornell Nanofabrication Facility/National Nanofabrication Center. This work also made use of the Cornell Center for Materials Research Facilities supported by the National Science Foundation under Award No. DMR-1120296.

[1]K. S. Novoselov, A. K. Geim, S. V. Morozov, D. Jiang, Y. Zhang, S. V. Dubonos, I. V. Grigorieva, and A. A. Firsov, Science **306**, 666 (2004).
[2]C. Berger, Z. Song, T. Li, X. Li, A. Y. Ogbazghi, R. Feng, Z. Dai, A. N. Marchenkov, E. H. Conrad, P. N. First, and W. A. de Heer, J. Phys. Chem. B **108**, 19912 (2004).
[3]A. H. Castro Neto, F. Guinea, N. M. R. Peres, K. S. Novoselov, and A. K. Geim, Rev. Mod. Phys. **81**, 109 (2009).
[4]I. W. Frank, D. M. Tanenbaum, A. M. van der Zande, and P. L. McEuen, J. Vac. Sci. Technol. B **25**, 2558 (2007).
[5]D. Garcia-Sanchez, A. M. van der Zande, A. San Paulo, B. Lassagne, P. L. McEuen, and A. Bachtold, Nano lett. **8**, 1399 (2008).
[6]J. S. Bunch, S. S. Verbridge, J. S. Alden, A. M. van der Zande, J. M. Parpia, H. G. Craighead, and P. L. McEuen, Nano lett. **8**, 2458 (2008).

[7]X. Li, W. Cai, J. An, S. Kim, J. Nah, D. Yang, R. Piner, A. Velamakanni, I. Jung, E. Tutuc, S. K. Banerjee, L. Colombo, and R. S. Ruoff, Science **324**, 1312 (2009).
[8]Y. Lee, S. Bae, H. Jang, S. Jang, S.-E. Zhu, S. H. Sim, Y. I. Song, B. H. Hong, and J.-H. Ahn, Nano Lett. **10**, 490 (2010).
[9]R. S. Edwards and K. S. Coleman, Acc. Chem. Res. **46**, 23 (2013).
[10]X. Chen, K. Lee, D. Akinwande, G. F. Close, S. Yasuda, B. Paul, S. Fujita, J. Kong, and H.-S. P. Wong, IEEE Int. Electron Devices Meet. **2009**, 1–4.
[11]A. Behnam, A. S. Lyons, M. Bae, E. K. Chow, S. Islam, C. M. Neumann, and E. Pop, Nano Lett. **12**, 4424 (2012).
[12]S. K. Min, W. Y. Kim, Y. Cho, and K. S. Kim, Nat. Nanotechnol. **6**, 162 (2011).
[13]K. Kim, Z. Lee, B. D. Malone, K. T. Chan, B. Alemán, W. Regan, W. Gannett, M. F. Crommie, M. L. Cohen, and A. Zettl, Phys. Rev. B **83**, 245433 (2011).
[14]W. Zhu, T. Low, V. Perebeinos, A. A. Bol, Y. Zhu, H. Yan, J. Tersoff, and P. Avouris, Nano lett. **12**, 3431 (2012).
[15]E. Prada, P. San-Jose, and L. Brey, Phys. Rev. Lett. **105**, 106802 (2010).
[16]M. M. Fogler, A. H. Castro Neto, and F. Guinea, Phys. Rev. B **81**, 161408 (2010).
[17]Y. Xie, Y. Chen, X. L. Wei, and J. Zhong, Phys. Rev. B **86**, 195426 (2012).
[18]Z. Yongping, W. Ning, F. Zheyong, X. Lanqing, and H. Zhigao, Nanotechnology **22**, 405701 (2011).
[19]D. Rainis, F. Taddei, M. Polini, G. León, F. Guinea, and V. I. Fal'ko, Phys. Rev. B **83**, 165403 (2011).
[20]A. Cresti, M. M. Fogler, F. Guinea, A. H. Castro Neto, and S. Roche, Phys. Rev. Lett. **108**, 166602 (2012).
[21]M. Currie, J. D. Caldwell, F. J. Bezares, J. Robinson, T. Anderson, H. Chun, and M. Tadjer, App. Phys. Lett. **99**, 211909 (2011).
[22]G. Kalita, L. Qi, Y. Namba, K. Wakita, and M. Umeno, Mater. Lett. **65**, 1569 (2011).
[23]N. Kurra, A. A. Sagade, and G. U. Kulkarni, Adv. Funct. Mater. **21**, 3836 (2011).
[24]S. Dhar, A. R. Barman, G. X. Ni, X. Wang, X. F. Xu, Y. Zheng, S. Tripathy, Ariando, A. Rusydi, K. P. Loh, M. Rubhausen, A. H. Castro Neto, B. Őzyilmaz, and T. Venkatesan, AIP Adv. **1**, 022109 (2011).
[25]J. H. Yoo, J. B. In, J. B. Park, H. J. Jeon, and C. P. Grigoropoulos, Appl. Phys. Lett. **100**, 233124 (2012).
[26]Y.-Q. Xu, A. Barnard, and P. L. McEuen, Nano Lett. **9**, 1609 (2009).
[27]P. Y. Huang, C. S. Ruiz-Vargas, A. M. van der Zande, W. S. Whitney, M. P. Levendorf, J. W. Kevek, S. Garg, J. S. Alden, C. J. Hustedt, Y. Zhu, J. Park, P. L. McEuen, and D. A. Muller, Nature **469**, 389 (2011).
[28]K. Kim, V. I. Artyukhov, W. Regan, Y. Liu, M. F. Crommie, B. I. Yakobson, and A. Zettl, Nano Lett. **12**, 293 (2012).
[29]C. Casiraghi, A. Hartschuh, H. Qian, S. Pliscanec, C. Georgia, A. Fasoli, K. S. Novoselov, D. M. Basko, and A. C. Ferrari, Nano Lett. **9**, 1433 (2009).
[30]Y. Lu, C. A. Merchant, M. Drndic, and A. T. Johnson, Nano lett. **11**, 5184 (2011).
[31]A. Barreiro, F. Borrnert, M. H. Rummeli, B. Buchner, and L. M. Vandersypen, Nano lett. **12**, 1873 (2012).
[32]K. Todd, H. Chou, S. Amasha, and D. Goldhaber-Gordon, Nano lett. **9**, 416 (2009).
[33]S. F. Shi, X. Xu, D. C. Ralph, and P. L. McEuen, Nano Lett. **11**, 1814 (2011).
[34]O. Cretu, A. R. Botello-Mendez, I. Janowska, C. Pham-Huu, J. C. Charlier, and F. Banhart, Nano lett. **13**, 3487 (2013).
[35]S. Nakaharai, T. Iijima, S. Ogawa, S. Suzuki, S. Li, K. Tsukagoshi, S. Sato, and N. Yokoyama, ACS Nano **7**, 5694 (2013).
[36]F. Prins, A. Barreiro, J. W. Ruitenberg, J. S. Seldenthuis, N. Aliaga-Alcalde, L. M. Vandersypen, and H. S. van der Zant, Nano Lett. **11**, 4607 (2011).
[37]B. Ozyilmaz, P. Jarillo-Herrero, D. Efetov, and P. Kim, Appl. Phys. Lett. **91**, 192107 (2007).
[38]B. Terrés, J. Dauber, C. Volk, S. Trellenkamp, U. Wichmann, and C. Stampfer, Appl. Phys. Lett. **98**, 032109 (2011).
[39]X. Li, X. Wang, L. Zhang, S. Lee, and H. Dai, Science **319**, 1229 (2008).
[40]M. Evaldsson, I. V. Zozoulenko, H. Xu, and T. Heinzel, Phys. Rev. B **78**, 161407 (2008).
[41]S. Masubuchi, M. Arai, and T. Machida, Nano Lett. **11**, 4542 (2011).
[42]A. Castellanos-Gomez, M. Barkelid, A. M. Goossens, V. E. Calado, H. S. J. Van Der Zant, and G. A. Steele, Nano Lett. **12**, 3187 (2012).